



ELSEVIER

Catalysis Today 64 (2001) 205–215



www.elsevier.com/locate/cattod

Experimental procedure for kinetic studies on egg-shell catalysts The case of liquid-phase hydrogenation of 1,3-butadiene and *n*-butenes on commercial Pd catalysts

N.O. Ardiaca^{a,b}, S.P. Bressa^{a,b}, J.A. Alves^{a,b}, O.M. Martínez^{a,b}, G.F. Barreto^{a,b,*}

^a *Centro de Investigación y Desarrollo en Procesos Catalíticos (CINDECA),*

Universidad Nacional de La Plata y Consejo Nacional de Investigaciones Científica y Técnicas, La Plata, Argentina

^b *Programa de Investigación y Desarrollo en Ingeniería de Reactores (PROIRQ), Facultad de Ingeniería,
Universidad Nacional de La Plata, La Plata, Argentina*

Abstract

A study of the liquid-phase hydrogenation of 1,3-butadiene on commercial Pd/Al₂O₃ catalysts of the “egg-shell” type has been performed. Experimental conditions (40°C, 4 atm and high conversion of the di-olefin) were selected in accordance to industrial operating conditions employed for selective hydrogenation of 1,3-butadiene. Three experimental schemes were tested: a slurry reactor, a rotating-basket reactor, and a recirculation system with an external fixed-bed reactor. Significant drawbacks shown by the two former devices were mainly derived from the very high activity and the egg-shell structure of the catalysts. Instead, the recirculation system was found to be an excellent alternative.

Although Pd is present only within a very thin external layer (around 50–250 μm), strong diffusion effects impairing selectivity were observed. Plausible kinetic expressions corresponding to nine series-parallel overall reactions are derived from a mechanistic model. To deal with this network of fast reactions, a rather complex set of computational and predictive tools were employed. A worked out example from several replicates demonstrates the capability of both, experimental and data analysis procedures, for inferring kinetic parameters of the proposed model. © 2001 Elsevier Science B.V. All rights reserved.

Keywords: Multiphase reactions; Selective hydrogenation; Laboratory reactors; 1,3-Butadiene; Pd/Al₂O₃ catalyst

1. Introduction

The purification of olefin rich C₄'s cuts, mainly from FFC, is conveniently carried out by selective hydrogenation of undesirable amounts of 1,3-butadiene and acetylenic compounds. 1-Butene employed either as monomer or as co-monomer in the pro-

duction of LLDP requires a nearly complete conversion of the di-olefin and acetylenics up to 10–20 ppm. It is not feasible to obtain this high purity condition by means of distillation due to the fact that di-olefin and mono-olefin have similar boiling points.

Purification of C₄'s cuts is industrially carried out in fixed catalytic beds with the liquid hydrocarbon mixture and H₂ flowing concurrently either in down or up flow at temperature ranging from ambient levels to about 50–60°C and total pressure high

* Corresponding author. Tel.: +54-221-4-211353;

fax: +54-221-4-254277.

E-mail address: barreto@dalton.quimica.unlp.edu.ar (G.F. Barreto).

enough to maintain the hydrocarbons in liquid phase [1].

Most commercial catalysts are manufactured by impregnating with the active agents only an external thin layer (around 50–250 μm) of alumina pellets. Different pellet geometries are found (spherical, trilobe, tablet) and sizes are of a few millimetres. The overall Pd content ranges typically within 0.1–0.5% (w/w). Pd is usually promoted by a second metal [2].

Palladium is known to be quite effective for selective hydrogenation due to the fact that the reactions of olefins are inhibited by the stronger adsorption of acetylenics compounds and 1,3-butadiene [3]. Nevertheless, if due to diffusion limitations the concentration of these contaminants rapidly drops inside the catalyst, the olefins will have the chance to react. Therefore, egg-shell catalysts [4] are employed to alleviate diffusion limitations.

Contrary to expectation from the previous discussion, we have found experimentally that fresh egg-shell commercial catalysts effectively show severe diffusion limitations for typical operating conditions. By a fresh catalyst we mean a sample being under reaction conditions by several hours instead of the initial performance evaluated in term of minutes.

A kinetic investigation, performed as close to the industrial operating conditions as possible, will allow us to forge a tool which can be applied to identify the main factors affecting the conversion and selectivity in commercial reactors. The kinetics studies available in the literature have been carried out either in gaseous phase [5,6] or with laboratory catalysts [7].

It is the aim of this contribution to describe our experience and present some conclusions in developing experimental and analytical procedures to study the kinetics of egg-shell commercial catalysts for selective hydrogenation of liquid C_4 's cuts.

The paper is organized as follows. The definitive experimental set-up and experimental procedure will be first described. The analysis carried out for choosing the type of experimental reactor on the light of experimental evidence is then discussed. A kinetic model based on elementary steps will also be presented. After describing the numerical tools for regression analysis, the results obtained from a set of experiments are analysed. Conclusions and significance are finally presented.

2. Experimental

2.1. Catalysts and other materials

Unless stated the contrary, experiments reported in this paper were performed on a commercial catalyst with Pd at 0.2% (w/w) impregnated on the 230 μm external layer of alumina spheres of 2.34 mm in diameter. The void fraction of this catalyst is 0.4 and presents a specific surface of 71 m^2/g .

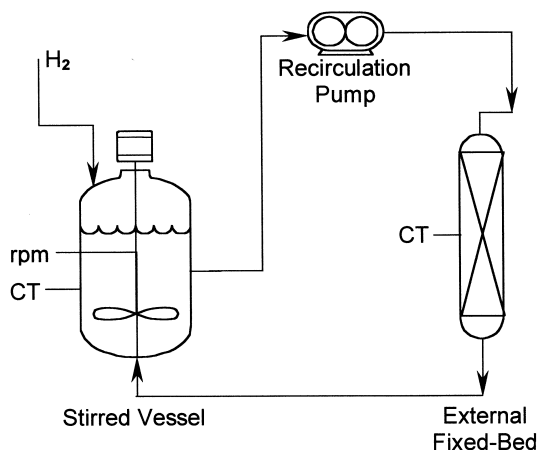
H_2 (99.999%) and N_2 (99.999%) were purified from water and oxygen by passing the streams through a guard bed of the same catalyst followed by a bed of 4A molecular sieve and an oxygen trap. Hydrocarbons employed were 1,3-butadiene (99.0%), 1-butene (99.0%), propane (99.99%) and *n*-hexane (HPLC, 97%), which were contacted with 4A molecular sieve first to their use.

2.2. Experimental set-up and operation

Batch type experiments with respect to the unsaturated reactants were planned at the outset of this investigation because of simplicity, economy and the amount of information provided by each run. The batch volume was around 100 ml and the catalyst weight necessary for carrying out the kinetic tests during 2–4 h was about 1 g. Except for the first run, which was faster and always discarded, the next runs (up to four or five) with a given catalyst sample showed satisfactorily stable performance.

As transient processes within the catalytic layer or on the catalytic surface are expected to take place in seconds or at most minutes [8], the time scale chosen for the batch experiments is large enough to consider that observed composition changes can be attributed to quasi-stationary reaction rates.

The main components of the experimental set-up finally adopted for the kinetic study are sketched in Fig. 1. The 100 ml stirred vessel is part of a commercially available system for reaction tests. This vessel contains most of the liquid mixture in the loop. *n*-Hexane is employed as an inert solvent to facilitate the loading of the C_4 reactants and the manipulation of the samples for chromatographic analysis. The operating pressure, P_T , is maintained by feeding H_2 through a pressure regulator. The level of H_2 partial pressure, P_{H_2} , can be chosen within a wide



CT: Temperature Control
rpm: Agitation Speed Control

Fig. 1. Experimental set-up: recirculation system with an external fixed-bed reactor.

range (from about 0.3 atm) and maintained essentially constant during the run by loading a proper amount of propane, which allows to fix P_{H_2} as the difference between P_T and sum of hydrocarbon partial pressures.

The impeller, provided by the manufacturer of the stirred reactor system, is a special device designed for stirring and at the same time dispersing vigorously the gas into the liquid. This device consists in a turbine with six flat-blades mounted at the edges of two disks concentric with the shaft. The shaft is hollow and shows lateral orifices drilled at the level of the freeboard and at the level of the chamber delimited by the two disks. When the impeller rotates, the gas is drawn from the freeboard and dispersed into the liquid. It was checked that above 1000 rpm, the mass exchange between the swarm of bubbles and the liquid is high enough to maintain the latter saturated by hydrogen at reaction conditions.

The catalyst sample, in its original size, is placed in an external stainless steel of $\frac{1}{4}$ in. tube with a jacket in which water at the same temperature of the stirred vessel is circulated. Temperature in the stirred vessel is controlled through an electrical heater around the vessel.

The reacting liquid is circulated through the catalyst bed by a gear micro-pump at 700 ml/min. This flow is high enough to obtain a negligible chemical

conversion per pass through the bed. Therefore, the whole system may be considered at uniform composition. Also, the very high particle Reynolds numbers resulting in the fixed bed ($Re_p \cong 2000$) allows to reduce interparticle mass transfer limitations to a minimum, as checked experimentally and by the use of correlations.

Liquid samples were analysed by gas chromatography employing a $2\text{ m} \times 2\text{ mm}$ column packed with 0.19% picric acid on 80–100 mesh Graphpac and an FID detector. The separation of propane, 1,3-butadiene, 1-butene, *cis*-2-butene, *trans*-2-butene and *n*-butane is achieved at ambient temperature. Samples of the vapour phase were also analysed separately to check the constancy of H_2 partial pressure.

2.3. Catalyst treatment

The catalyst samples were treated (for reduction finishing) in the same bed described before employing a mixture of N_2 (78%) and H_2 (22%) at 54°C for 9 h. Preliminary tests showed that if in the course or after the kinetic experiments the catalyst sample gets into contact with moisture, its catalytic activity drops significantly. This is the reason for the precautions taken to eliminate humidity or O_2 (which produces H_2O in the presence of H_2) in the gases and hydrocarbons employed for the experimental runs.

3. Selection of the experimental configuration

The slurry reactor is considered the most typical system for testing catalysts for liquid or gas–liquid reactions [9]. Therefore, the first tests were performed by working with a slurry suspension of milled catalyst samples (500–700 μm) in the stirred vessel described above, rather than employing the external fixed-bed.

It was found that with stirring speeds higher than 600 rpm a significant amount of catalyst dust (apparently produced by attrition during the tests) was found adhered to the walls of the vessel head in contact with the gas phase under operation. It is recalled that high rotational speed should be employed to maintain the liquid saturated with H_2 . A preliminary analysis of the data thus obtained revealed the existence of strong diffusion limitations within the active layer. These observations not only apply to the specific catalyst

chosen to continue the study, but also to samples of other five commercial catalysts.

As it will be shown later, particle size should be reduced to less than about 10 μm to eliminate completely the diffusion effects. Working with particles less than 10 μm did not appear as a practically convenient alternative. The already mentioned problem of dust adhesion at the vessel head was expected to become worse. Also, the reduced space available inside the small vessel would introduce the need of installing specially designed micro-filters for sampling and removing the liquid solution after each run. In any case, severe clogging of the filters may be expected by the presence of large amount of dust (note that size classification of the milled powder cannot be performed conventionally below 10 μm).

On the other hand, milling to more usual sizes, say 50–300 μm , will attenuate diffusion effects, but they will not be eliminated completely. The drawback of working with this range of sizes is that the sample will show a distribution of particle composition (active and inert zones), since the thickness of the original active layer is within that range. This feature will introduce uncertainties in evaluating the still existent diffusion effects, which in turn will be transferred to the estimation of kinetic parameters.

The decision adopted was working with the catalyst in its original size, in spite of having to incorporate the diffusion effects in the data analysis procedure. Nonetheless, this task is favoured by the fact that the geometrical configuration of the original catalyst particles is well defined.

New series of experiments were performed with two systems: one employing a rotating-basket reactor and the system with the external fixed-bed previously described (Section 2.2).

Four baskets holding the catalyst sample were employed in the first case. Due to the small dimensions of the vessel, it was necessary to construct a new impeller to install the baskets while keeping the gas dispersion and stirring actions described in Section 2.2 for the original device. In particular, the height of the chamber delimited by the two disks (Section 2.2) was reduced and the external diameter of the device increased, to provide room for mounting the baskets. They were fixed on the top of the upper disk and a third perforated disk above the baskets was used to maintain the catalyst particles in place. The baskets

are nearly cubic: 8.5 mm radial side, 11 mm tangential side and 8 mm high. The baskets can accommodate up to 1.5 g of catalyst. This amount is necessary to perform the kinetic tests in a few hours (Section 2.2).

The outstanding results from the tests can be appreciated with the help of Fig. 2, where the consumption of 1-butene (the only unsaturated reactant initially present in this particular run) from both systems, spinning basket reactor and external fixed-bed reactor, is compared. The slower rate obtained with the rotating baskets can be ascribed to relatively low liquid flow through the baskets, causing a concentration drop with respect to the liquid bulk.

This behaviour is against expectation, as the spinning basket reactor is recommended to minimize interfacial gradient effects. An explanation for the observed performance can be found in the design of the baskets. Each of them holds around 50 particles of those employed for the data in Fig. 2. Four or five layers of particles (2.34 mm in diameter) builds along the tangential dimension (11 mm) of each basket. The best arrangement arises when the basket contains only one layer (as actually described by Carberry [10] in his pioneer work introducing the spinning basket reactor). Pereira and Calderbank [11] showed that the mass transfer coefficient to the particles in the basket significantly decreases as the number of layers increases due to a pressure drop effect. The small radial dimension of our device is another drawback (the innermost side of the basket is at about 5 mm from the shaft axis and the outermost side at about 15 mm). The tangential velocities are, therefore, relatively small and highly variable. Pereira and Calderbank [11] showed that the local mass transfer coefficient strongly decreases as the radial position decreases.

No substantial modification of the design was envisaged while keeping the constraints imposed by the size of the vessel and the desirable amount of catalyst sample.

As regards the results in Fig. 2 for the system with the external fixed-bed, it was already commented that the high recirculation rate allows proper fluid-to-particle mass transfer rates, as needed by the fast catalytic system studied. The estimated differences between catalyst-surface and liquid-bulk concentrations were at most 5% (see Sections 4 and 5 for more details about these evaluations).

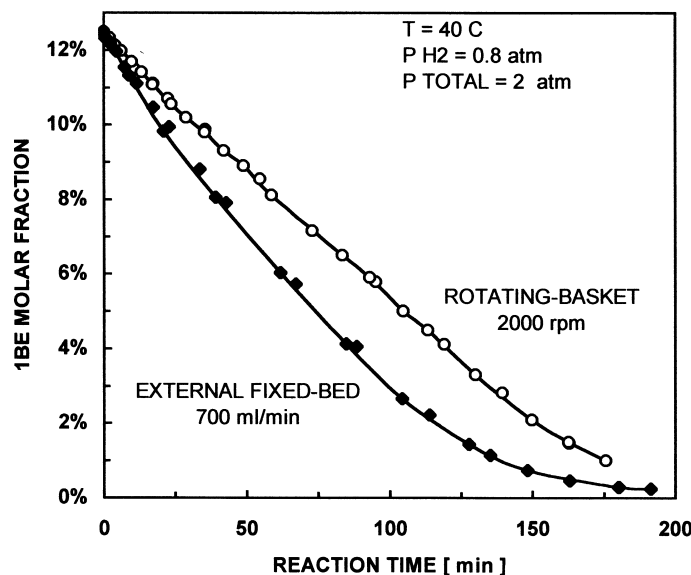


Fig. 2. Rate of consumption of 1-butene: comparison between the rotating-basket reactor and the recirculation system. Liquid volume: 108 ml, $M_{\text{cat}} = 1$ g.

To conclude this section, it is important to remark that the recirculating system employed shows additional advantages for batch tests. The total liquid volume drained from the system for a correct sampling can be minimized, as the recirculating stream is used for sweeping the sampling chamber. Also, the catalyst is isolated while the batch is being prepared and the operating conditions are set; hence a neat start of the reaction test is achieved.

4. Kinetic model

Considering that butadiene is the only impurity present in the system, the overall set of reactions taking place can be sketched as in Fig. 3, where BD \equiv 1, 3-butadiene, 1BE \equiv 1-butene, cBE \equiv *cis*-2-butene, tBE \equiv *trans*-2-butene and BA \equiv *n*-butane. The only possible reaction not considered is the direct hydrogenation of BD to BA, which does not occur in practice [12]. The hydrogenation reactions are irreversible under normal operating conditions and the thermodynamic stability ranking for the *n*-butenes isomers is tBE > cBE > 1BE.

We will present in this section rate expressions for the set of overall reactions defined in Fig. 3. These

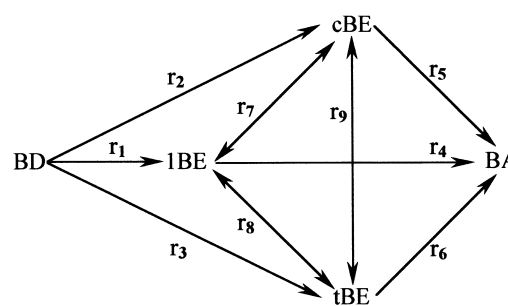


Fig. 3. Overall reaction network.

expressions have been derived from a catalytic mechanism. Although this mechanism is at present being tested with a large set of experimental data, we can at least confirm that the rate expressions derived from it are able to capture the underlying kinetic characteristics observed in our experiments, consisting in monitoring bulk composition of the unsaturated species in the course of the reaction.

Due to the fact that the proposed mechanism is still under analysis and that for the purpose of the present contribution we only need suitable overall kinetic expressions, we will just highlight here its essential features. The proposed mechanism consists of 15 elementary steps, which were written under

the following hypothesis:

- dissociative adsorption of H₂ on sites different to those involved with hydrocarbons is assumed, i.e. noncompetitive adsorption is adopted;
- the unsaturated hydrocarbons adsorb on sites “*” forming π-adsorbed surface intermediates;
- the BD π-adsorbed intermediate adds a hydrogen ad-atom to produce a surface intermediate C₄H₇^{*}, which is the common precursor to the formation of the three *n*-butenes;
- the 1BE π-adsorbed intermediate, by adding a hydrogen ad-atom, can lead to two different intermediates: the 1-butyl (C₄H₉^{*}) and the 2-butyl (C₄H₉^{*}) adsorbed radicals;
- the *cis*–*trans* isomerization reactions and the migration of the double bond proceed through the dehydrogenation of the radical C₄H₉^{*};
- the hydrogenation of the radicals C₄H₉^{*} and C₄H₉^{*} leads to the formation of *n*-butane.

The steps for the hydrogenation of BD are taken from models proposed in the literature [5], while the hypothesis for the *n*-butene reactions and H₂ adsorption are the results of the analysis of previous experiments in vapour phase [13].

Additionally, the following assumptions are made in deriving the overall kinetic expressions from the elementary steps,

- all adsorption steps are equilibrated;
- the amount of sites “*” occupied by saturated hydrocarbons and by the radicals C₄H₇^{*}, C₄H₉^{*}, C₄H₉^{*} can be neglected.

From the proposed mechanism, the resulting steady-state rate expressions for the overall reactions defined in Fig. 3 are as follows:

$$r_1 = \frac{k_1 x_{\text{BD}} (x_{\text{H}_2})^{1/2}}{\text{DEN}_{\text{HC}} \text{DEN}_{\text{H}_2}}, \quad r_2 = \frac{k_2 x_{\text{BD}} (x_{\text{H}_2})^{1/2}}{\text{DEN}_{\text{HC}} \text{DEN}_{\text{H}_2}},$$

$$r_3 = \frac{k_3 x_{\text{BD}} (x_{\text{H}_2})^{1/2}}{\text{DEN}_{\text{HC}} \text{DEN}_{\text{H}_2}},$$

$$r_4 = \frac{k_4^{\text{I}} x_{1\text{BE}} x_{\text{H}_2}}{\text{DEN}_{\text{HC}} \text{DEN}_{\text{A}_{\text{H}_2}}} + \frac{k_4^{\text{II}} x_{1\text{BE}} x_{\text{H}_2}}{\text{DEN}_{\text{HC}} \text{DEN}_{\text{B}_{\text{H}_2}}},$$

$$r_5 = \frac{k_5 x_{\text{cBE}} x_{\text{H}_2}}{\text{DEN}_{\text{HC}} \text{DEN}_{\text{B}_{\text{H}_2}}},$$

$$r_6 = \frac{k_6 x_{1\text{BE}} x_{\text{H}_2}}{\text{DEN}_{\text{HC}} \text{DEN}_{\text{B}_{\text{H}_2}}},$$

$$r_7 = \frac{k_7 (x_{\text{H}_2})^{1/2}}{\text{DEN}_{\text{HC}} \text{DEN}_{\text{B}_{\text{H}_2}}} \left[x_{1\text{BE}} - \frac{x_{\text{cBE}}}{K_7^{\text{eq}}} \right],$$

$$r_8 = \frac{k_8 (x_{\text{H}_2})^{1/2}}{\text{DEN}_{\text{HC}} \text{DEN}_{\text{B}_{\text{H}_2}}} \left[x_{1\text{BE}} - \frac{x_{1\text{BE}}}{K_8^{\text{eq}}} \right],$$

$$r_9 = \frac{k_9 (x_{\text{H}_2})^{1/2}}{\text{DEN}_{\text{HC}} \text{DEN}_{\text{B}_{\text{H}_2}}} \left[x_{\text{cBE}} - \frac{x_{1\text{BE}}}{K_9^{\text{eq}}} \right]$$

where

$$\text{DEN}_{\text{HC}} = 1 + K_{\text{BD}}^{\text{ad}} x_{\text{BD}} + K_{1\text{BE}}^{\text{ad}} x_{1\text{BE}} + K_{\text{cBE}}^{\text{ad}} x_{\text{cBE}} + K_{1\text{BE}}^{\text{ad}} x_{1\text{BE}},$$

$$\text{DEN}_{\text{H}_2} = [1 + (K_{\text{H}_2}^{\text{ad}} x_{\text{H}_2})^{1/2}],$$

$$\text{DEN}_{\text{A}_{\text{H}_2}} = \text{DEN}_{\text{H}_2} [1 + \alpha (K_{\text{H}_2}^{\text{ad}} x_{\text{H}_2})^{1/2}],$$

$$\text{DEN}_{\text{B}_{\text{H}_2}} = \text{DEN}_{\text{H}_2} [1 + \beta (x_{\text{H}_2})^{1/2}]$$

$$\beta = \frac{k_5}{k_9 (1 + k_7/k_8) + k_7/K_7^{\text{eq}}}$$

K_j^{ad} is the adsorption constant for species “*j*” and K_i^{eq} is the thermodynamic equilibrium constant for reaction “*i*”.

The resulting kinetic constants, $k_1, k_2, k_3, k_4^{\text{I}}, k_4^{\text{II}}, k_5, \dots, k_9$, are actually expressed in terms of the kinetic coefficients of the elementary steps. From these expressions, it is possible to conclude that only eight of those constants can take independent values. The constants k_4^{II} and k_6 can be chosen as those being dependent. The relating relationships are

$$k_4^{\text{II}} = \frac{k_5 k_8}{k_9}, \quad k_6 = \frac{k_5 k_8}{k_7 K_9^{\text{eq}}}$$

Therefore, the above kinetic model presents fourteen independent parameters k_i ($i = 1, 2, 3, 5, 7, 8, 9$), k_4^{I} , α and the adsorption constants $K_{\text{BD}}^{\text{ad}}, K_{1\text{BE}}^{\text{ad}}, K_{\text{cBE}}^{\text{ad}}, K_{1\text{BE}}^{\text{ad}}$ and $K_{\text{H}_2}^{\text{ad}}$. Units employed in the above rate expressions are moles per second and per unit weight of the active catalytic layer.

5. Data analysis

The available information for each experimental run is the liquid composition (expressed in terms of mole

fraction $x_{j,\text{bulk}}$ for each unsaturated species j) at a set of reaction times. Given the values of $x_{j,\text{bulk}}$, the number of moles of each species j can be evaluated as

$$N_j = N_T x_{j,\text{bulk}} \quad (1)$$

where N_T is the total number of moles.

We have neglected in the treatment the amount of unsaturated species in the vapour phase, as this was checked to be always less than 1%. Instead, the liquid volume extracted for sampling was about 10–20% of the initial batch. Since this percentage is not negligible, the number of moles N_T was corrected after each sample.

In order to estimate the kinetic parameters of the model outlined in Section 4, the basic approach consists of trying a set of values for the kinetic parameters, evaluating the composition as a function of the reaction time and comparing predicted and measured values of N_j . This is known as an integral analysis.

We will consider with certain detail the second step, i.e. how the composition is evaluated at any desired reaction time t . As the catalytic bed operates under essentially uniform bulk liquid conditions (due to high recirculation flow), the conservation equations employed for the unsaturated species during each run were

$$\frac{dN_j}{dt} = M_{\text{cat}} \bar{r}_j \quad (2)$$

where \bar{r}_j is the observed rate of chemical production of species j per unit mass of catalyst sample M_{cat} .

Eq. (2) can be numerically integrated with any code for solving ordinary first-order differential equations. At any time during the integration, we should evaluate \bar{r}_j from the instantaneous values of N_j , or equivalently, from $x_{j,\text{bulk}}$ (Eq. (1)). To this end, \bar{r}_j is calculated by taking into account the external and internal mass transport limitations. The conservation balances inside the active catalytic layer have been written as

$$D_j C_T \frac{d^2 x_j}{dz^2} = -L^2 \rho_{\text{cat}} r_j \quad (3)$$

where z is the dimensionless coordinate inside the layer, $z = z'/L$ (L is the thickness of the active catalytic layer), r_j the rate of chemical production of j per unit mass of active catalytic layer, evaluated at z , x_j the mole fraction of j at z , C_T the total molar concen-

tration of the liquid, D_j the effective diffusivities of j inside the active layer, and ρ_{cat} the particle density.

In writing Eq. (3), it was considered that L is small enough to ignore curvature effect and that mass transport inside the catalyst can be described by a Fick type expression (this assumption is valid as n -hexane is present in the liquid solution in large excess). Also, it was checked that heat transfer from the particles to the liquid stream was fast enough to maintain uniform temperature.

The production rates r_j and the overall reaction rates given in Section 4 are related stoichiometrically. For instance, for 1-butene, $r_{1\text{BE}} = r_1 - r_7 - r_8 - r_9$ (see Fig. 3).

Boundary conditions for Eq. (3) are:

$$D_j \frac{dx_j}{dz} = L h_j (x_j - x_{j,\text{bulk}}) \quad \text{at} \\ z = 0 \text{ (catalyst surface)} \quad (4a)$$

$$\frac{dx_j}{dz} = 0 \quad \text{at } z = 1 \text{ (end of the active layer)} \quad (4b)$$

where h_j is the mass transfer coefficient between the particle surface and the liquid bulk.

Eq. (3) along with their boundary conditions ((4a) and (4b)) should be solved at any reaction time from the known values of $x_{j,\text{bulk}}$ and the trial set of kinetic parameter values. Once this task has been performed, the resulting field of mole fractions inside the layer, x_j , allows to compute

$$\bar{r}_j = \left(\int_0^1 r_j dz \right) \frac{L S_{\text{cat}} \rho_{\text{cat}}}{M_{\text{cat}}} \quad (5)$$

from which the integration of Eq. (2) can proceed. In Eq. (5), S_{cat} is the external area of the catalyst sample.

The regression analysis to evaluate the best estimates of the intrinsic kinetic parameters has been performed by the pack of routines GREGPAK [14] employing the multiresponse mode. Integration of Eq. (2) has been performed by the routine DDASAC included in GREGPAK.

A numerical algorithm was specifically developed [15] to solve Eqs. (3), (4a) and (4b). This step should be performed as efficiently as possible, since it takes most of the computing time. This task is not trivial, as the strong diffusion limitation generates very steep internal profiles for some reactants, the kinetic expressions (Section 4) are highly non-linear and they

strongly couple the individual conservation balances (3). The solution should be performed many times for the integration of Eq. (2) (hundred is a typical value) for each run and for each trial set of kinetic parameters.

Effective diffusivities inside the catalyst were evaluated with a tortuosity factor of 2, obtained from previous evaluations [13]. The hydrogen molar fraction $x_{\text{H}_2, \text{bulk}}$ was evaluated from the known vapour-phase composition assuming phase equilibrium. The Soave–Redlich–Kwong EOS with MHSV mixing rules [16] and modified UNIFAC parameters [17] was employed to this end. The mass transfer coefficients h_j were evaluated from the correlation given by Gunn [18].

6. Results and discussion

An example of the results obtained for a set of experimental data will now be presented. The data corresponds to six replicates of different catalyst samples, starting with BD as the only reactant (BD alone can open the whole reaction network sketch in Fig. 3). Experimental conditions were: initial composition $x_{\text{BD}}^0 \cong 0.02$, $P_{\text{T}} = 4.1$ atm, $P_{\text{H}_2} = 3.25$ atm, $T = 40^\circ\text{C}$ and 0.8 g of catalyst in each sample. The experimental data for BD, 1BE, BA and tBE are shown in Fig. 4a and b. It can be observed that the dispersion of the data is satisfactorily low.

Given the fact that only one initial composition is employed in the replicates analysed here, it becomes clear that only a few parameters can be estimated with statistical significance. In particular, the adsorption constants of the *n*-butenes and H_2 ($K_{1\text{BE}}^{\text{ad}}$, $K_{\text{cBE}}^{\text{ad}}$, $K_{\text{tBE}}^{\text{ad}}$, $K_{\text{H}_2}^{\text{ad}}$) and parameter α could be set equal to zero without any consequence for the quality of the agreement between data and model estimates. This is due to the low content of *n*-olefins in the course of the experiments and to a fix value of P_{H_2} . The optimal values of the remaining parameters are listed in Table 1. Out of them, k_1 (BD to 1BE),

k_3 (BD to tBE), k_8 (tBE to BA) and the BD adsorption constant $K_{\text{BD}}^{\text{ad}}$ could be inferred with statistical significance (their linearized 95% confidence limits are about 10%). The other parameters present large confidence limits and high degree of correlation between themselves. They are mainly concerned with reactions producing or consuming cBE, which shows the lowest level of concentration (its maximum value is about 0.25% on molar basis).

Out of the four parameters determined with statistical significance, three are associated to the 1,3-butadiene reactions. It is not surprising that the parameters associated with the reactions consuming the three *n*-butene isomers could not be determined accurately, as those species are generated from the hydrogenations of BD. Tests with a set of suitable initial composition are needed to proceed with the kinetic analysis. This task is presently being carried out. The important point to remark here is that experimental and data analysis procedures allow a precise estimation of the parameters (those of BD) suitably associated with the experimental conditions (only BD initially present).

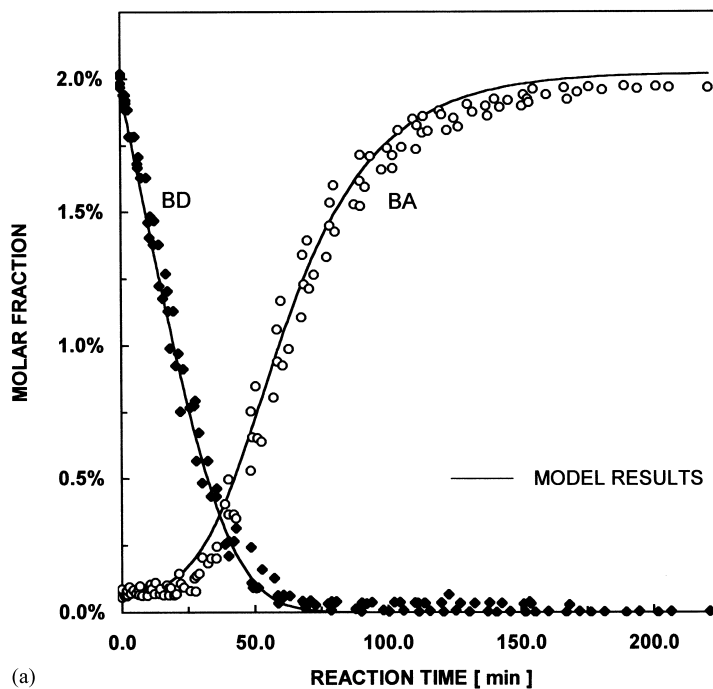
The results from the model, also presented in Fig. 4, produce a good fit for the experimental data. The fit for cBE (not shown in Fig. 4) is also as good as those of 1BE and tBE, in spite of the uncertainty of its related kinetic parameters.

The estimated concentration profiles of H_2 , 1BE and BD inside the catalyst layer ($z = 1$ corresponds to the end of the 230 μm active layer) for two reaction times are presented in Fig. 5a and b.

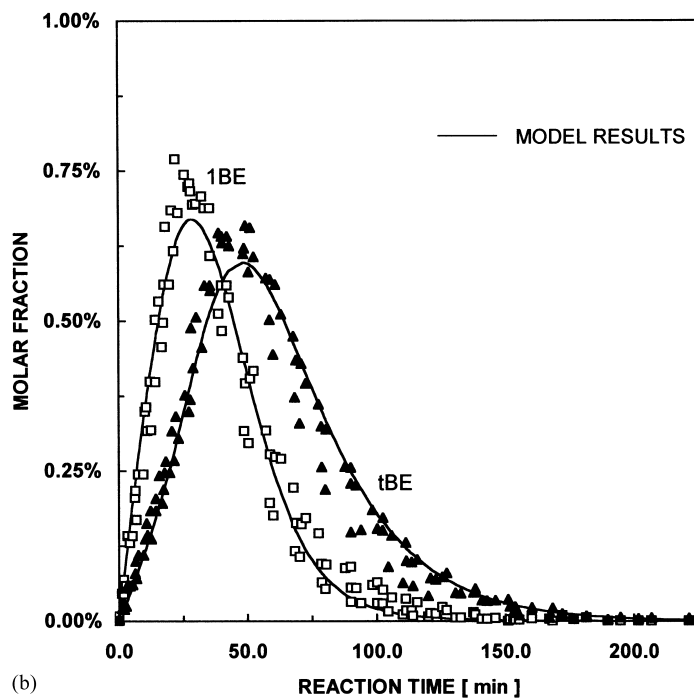
At the shorter time (10 min), H_2 is the diffusionally limiting reactant and is completely consumed at about 20% of the active layer. At these conditions, the relatively large BD concentrations can inhibit almost completely the 1BE consumption reactions. We employ the term diffusionally limiting reactant to stress the fact that diffusivity of H_2 is about four times those of the hydrocarbons. As the product of diffusivity and liquid-bulk concentration defines which reactant will

Table 1
Optimal values of the kinetic parameters ($[k_i] = \text{mol s}^{-1} \text{g}^{-1}$ active layer)

$k_1 = 4.14 \pm 5.31 \times 10^{-1}$	$k_2 = 3.44 \times 10^{-3}$	$k_3 = 8.31 \times 10^{-1} \pm 1.43 \times 10^{-1}$	$k_4^1 = 3.44 \times 10^{-1}$
$k_5 = 3.14$	$k_7 = 1.35 \times 10^{-1}$	$k_8 = 8.45 \times 10^{-1} \pm 9.84 \times 10^{-2}$	$k_9 = 2.84$
$K_{\text{BD}}^{\text{ad}} = 1067 \pm 185.0$			



(a)



(b)

Fig. 4. Comparison between experimental and model predicted composition as a function of reaction time.

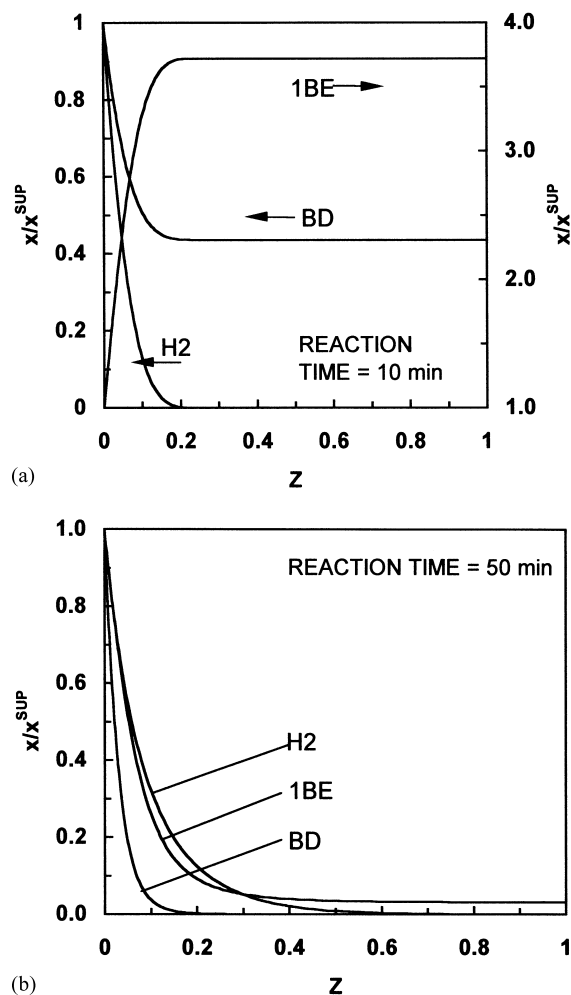


Fig. 5. Composition profiles inside the active layer. x/x^{sup} are the molar fractions relative to the value at the catalyst surface. Surface values: (a) $x_{\text{BD}}^{\text{sup}} = 1.45 \times 10^{-2}$, $x_{1\text{BE}}^{\text{sup}} = 3.91 \times 10^{-3}$, $x_{\text{H}_2}^{\text{sup}} = 2.33 \times 10^{-3}$; (b) $x_{\text{BD}}^{\text{sup}} = 1.04 \times 10^{-3}$, $x_{1\text{BE}}^{\text{sup}} = 4.16 \times 10^{-3}$, $x_{\text{H}_2}^{\text{sup}} = 2.38 \times 10^{-3}$.

be first depleted, the distinction from the stoichiometrically limiting reactant should be stressed.

At 50 min, the overall BD conversion is about 95% (its concentration has dropped to about 1000 ppm in the liquid bulk). Now, BD has become the diffusionally limiting reactant instead of H_2 . Simultaneously, all reactions are intrinsically faster, as a consequence of a lower BD inhibition term. At about one-tenth of the active layer thickness BD is almost depleted, leaving the chance for 1BE consumption reactions to take

place with the help of the excess H_2 . The estimated external transport limitations were always relatively low. The largest difference between catalyst-surface and liquid-bulk concentrations was about 5%.

Further calculations show that even reducing the active catalyst layer to the size of $10 \mu\text{m}$, diffusion effects still persist. These results confirm that the slurry reactor is not suitable to carry out a kinetic study with the present type of catalysts.

7. Final remarks and conclusions

Three conventional experimental techniques for the kinetic study of the liquid-phase hydrogenation of 1,3-butadiene and *n*-butenes on commercial Pd catalysts have been discussed: the slurry, the rotating-basket, and the recirculation reactors. The drawbacks shown by the two former systems are mainly derived from the very high activity and the structure (egg-shell type) of the catalyst employed. The selected recirculation system, using a stirred vessel for saturation and temperature control, was found to be a very good alternative to eliminate the uncertainties introduced by the other systems. It is believed that the experience detailed here for our particular system can also be useful for testing many other liquid, or particularly gas-liquid, fast catalytic reactions.

The system studied here presents, apart from the high reaction rates, a complex reaction network. These features introduce the need of employing an involved set of computational and predictive tools for data analysis. The example worked out in the text from several replicates allows drawing several conclusions. On one hand, it demonstrates the capability of both, experimental and data analysis procedures, for inferring the parameters of a plausible kinetic model outlined here. On the other hand, the strong diffusion limitations inside the active layer of the catalyst were clearly revealed.

The last conclusion shows important practical implications for industrial processes employing selective hydrogenation of C_4 olefin rich cuts. The presence of H_2 in excess to the amount required to deplete the impurities inside the catalyst will automatically activate the reactions of the *n*-butenes. It can be foreseen that a detailed knowledge of the kinetic behaviour will be most important in choosing operating conditions to maintain acceptable levels of olefin losses. It can be

argued that the design of commercial catalysts should not introduce such diffusion limitation. However, a lower initial activity (using less Pd content) would surely shorten the time of the catalyst under continuous service without regeneration or replacing. These catalysts are known to lose activity by heavy residues on the catalyst (green oil) [2]. A daily loss of 1% in activity would lead after 2 years to about one thousandth of the fresh catalyst activity. For an analysis of the global strategy, the presence of acetylenic compounds (i.e. 1-butyne) should not be avoided. They are expected not to pose any further problem about selectivity, but they are hydrogenated at a rate significantly lower than 1,3-butadiene [19]. Therefore, the activity level will be important to avoid very high catalyst loading.

Acknowledgements

The authors wish to thank the assistance of the following Argentinean institutions: ANPCyT-SECyT (PICT No. 00227), CONICET (PIP96 No. 4791, PEI97 No. 0524), and UNLP (PID No. 11/I058, Fellowship to NOA). JAA, OMM and GFB are members of CONICET, SPB is member of CIC PBA.

References

- [1] M. Derrien, in: L. Cerveny (Ed.), *Studies Surface Science Catalyst*, Vol. 27, Elsevier, Amsterdam, 1986, p. 613 (Chapter 18).
- [2] J.-P. Boitiaux, J. Cosyns, M. Derrien, G. Leger, *Hydrocarbon Process.* (March 1985) 51.
- [3] S. Hub, L. Hilaire, R. Touroude, *Appl. Catal.* 36 (1988) 307.
- [4] R. Krishna, S.T. Sie, *Chem. Eng. Sci.* 49 (1994) 4029.
- [5] J. Goetz, D.Yu. Murzin, M. Ulishenko, R. Touroude, *Chem. Eng. Sci.* 51 (1996) 2879.
- [6] P. Kripylo, F. Turek, *Chem. Technol.* 27 (1975) 605.
- [7] J.-P. Boitiaux, J. Cosyns, M. Derrien, G. Leger, in: *Proceedings of the AIChE Spring National Meeting*, Houston, TX, 1986, Paper No. 1453.
- [8] V.I. Bykov, V.I. Elokhin, A.N. Gorban, G.S. Yablonskii, in: R.G. Compton (Ed.), *Comprehensive Chemical Kinetics*, Vol. 32, Elsevier, Amsterdam, 1991.
- [9] P.L. Mills, P.A. Ramachandran, R.V. Chaudhari, *Rev. Chem. Eng.* 8 (1992) 1–2.
- [10] J.J. Carberry, *Ind. Eng. Chem.* 56 (1964) 39.
- [11] J.R. Pereira, P.H. Calderbank, *Chem. Eng. Sci.* 30 (1975) 167.
- [12] J.-P. Boitiaux, J. Cosyns, E. Robert, *Appl. Catal.* 35 (1987) 193.
- [13] S.P. Bressa, O.M. Martínez, G.F. Barreto, in: *Proceedings of the 11th Jornadas Argentinas de Catálisis*, San Luis, Argentina, September 28–October 1, 1999, Paper Nos. 7 and 8.
- [14] W.E. Stewart, M. Caracotsios, J.P. Sørensen, *AIChE J.* 38 (5) (1992) 641.
- [15] S.P. Bressa, N.J. Mariani, N.O. Ardiaca, G.D. Mazza, O.M. Martínez, G.F. Barreto, An algorithm for evaluating reaction rates of catalytic reaction networks with strong diffusion limitations, submitted for publication.
- [16] S. Dahl, S. Fredenslund, P. Rasmussen, *Ind. Eng. Chem. Res.* 30 (1991) 1936.
- [17] B. Larsen, P. Rasmussen, A. Fredenslund, *Ind. Eng. Chem. Res.* 26 (1987) 2274.
- [18] D.J. Gunn, *Int. J. Heat Mass Transfer* 21 (1978) 467.
- [19] S. Vasudevan, Ph.D. Thesis, L'Ecole Nationale Supérieure du Pétrole et des Moteurs, France, 1982.